JOURNAL OF APPROXIMATION THEORY 41, 64–86 (1984)

An Approach to Data Parametrization in Parametric Cubic Spline Interpolation Problems

SAMUEL P. MARIN

Mathematics Department, General Motors Research Laboratories, Warren, Michigan 48090-9055, U.S.A.

Communicated by Oved Shisha

Received April, 25, 1983

A new approach to the problem of parametrizing data in parametric cubic spline interpolation problems is discussed. Parametrizations $0 = t_0 < t_1 < \cdots < t_N = 1$ of K-dimensional data $\{\mathbf{z}_i\}_{i=0}^{N}$, $\mathbf{z}_i = (z_i^1, \ldots, z_i^K)$ are chosen by minimizing $\sum_{l=1}^{K} (1/\alpha_l^2) \int_0^1 (d^2\theta^l/dt^2)^2\, dt$, where $\theta^l(t)$ is the natural cubic spline with breakpoints $t_0, t_1, \ldots, t_N$ satisfying $\theta^l(t_i) = z_i^l$, $i = 0, \ldots, N$, and α_l, $l = 1, \ldots, K$, are positive numbers. This approach yields parametrizations which, by complementing the well-known smoothest interpolation property of natural cubic splines, leads to smoother component functions. The improvements are, in part, evidenced by reduced position overshoots and lower second derivatives. A closed form solution of the problem is derived for one-dimensional data. In higher dimensions the gradient projection method is used to obtain approximate numerical solutions. Geometric curve fitting problems and an example involving the design of a trajectory for a robot manipulator are used to illustrate the method.

1. INTRODUCTION

The purpose of this paper is to describe a new approach to the problem of parametrizing data in parametric cubic spline interpolation problems. We begin by introducing a constrained minimization problem whose solution yields the required data parametrization.

For K-dimensional data $\{\mathbf{z}_i\}_{i=0}^{N}$, $\mathbf{z}_i = (z_i^1, \ldots, z_i^K)$, and a partition $0 = t_0 < t_1 < \cdots < t_N = 1$ of $[0, 1]$, parametric interpolation within the space $S_0(t_0, t_1, \ldots, t_N)$ of natural cubic splines is accomplished by performing univariate interpolation K times. The result is a parametric curve passing through the given data, described by a vector valued function $\boldsymbol{\theta}(t) = (\theta^1(t), \ldots, \theta^K(t))$ whose components $\theta^l(t)$, $l = 1, \ldots, K$, are in $S_0(t_0, \ldots, t_N)$ and satisfy $\theta^l(t_i) = z_i^l$, $i = 0, \ldots, N$. If we fix the data $\{\mathbf{z}_i\}_{i=0}^{N}$ and define

0021-9045/84 $3.00

$h_i = t_i - t_{i-1}$, $i = 1,..., N$, then the following function G of the mesh spacing vector $\mathbf{h} = (h_1,..., h_N)^T$ is a weighted measure of component smoothness

$$G(\mathbf{h}) = \sum_{l=1}^{K} \frac{1}{\alpha_l^2} \int_0^1 \left(\frac{d^2\theta^l}{dt^2} \right)^2 dt. \tag{1}$$

We delay specifying the weights α_l, $l = 1,..., K$, in (1) until Section 3. At this point we merely assume that they are positive. Our objective in parametrizing the points $\{\mathbf{z}_i\}_{i=0}^N$ will be to

$$\underset{\mathbf{h} \in B}{\text{minimize}}\ G(\mathbf{h}), \tag{2}$$

where

$$B = \left\{ \mathbf{h} = (h_1,..., h_N)^T \mid h_i \geqslant 0,\ \sum_{i=1}^{N} h_i = 1 \right\}. \tag{3}$$

The desired parametrization t_0^*, $t_1^*,..., t_N^*$ is then induced by a minimizing mesh spacing $\mathbf{h}^* = (h_1^*,..., h_N^*)^T$ according to

$$t_0^* = 0, \qquad t_i^* = t_{i-1}^* + h_i^*, \qquad i = 1,..., N. \tag{4}$$

Remark (Existence of Solutions). We assume throughout that the data satsify $z_i \neq z_{i+1}$, $i = 0,..., N-1$. This requirement implies that $G(\mathbf{h})$ becomes infinite if any component of $\mathbf{h}$ vanishes and, coupled with standard continuity and compactness arguments, gives the existence of a minimizing mesh spacing vector with $h_i > 0$, $i = 1,..., N$.

There are several issues, in addition to the classical notion of smoothness (see [1]) which are addressed by parametrizing data $\{\mathbf{z}_i\}_{i=0}^N$ in this way. We summarize these:

(i) In geometric applications ($K = 2$ or 3), it is often desired that the cubic spline interpolating curve $\{\boldsymbol{\theta}(t) \mid t \in [0, 1]\}$ conform in shape to the interpolating polygon $\{\boldsymbol{\phi}(t) \mid t \in [0, 1]\}$, where $\boldsymbol{\phi}(t)$ is the piecewise linear interpolant of the data. The smooth curve will conform to the associated polygon if the difference $\mathbf{e}(t) \equiv \boldsymbol{\theta}(t) - \boldsymbol{\phi}(t)$ is small. For each component $e^l(t) = \theta^l(t) - \phi^l(t)$ of $\mathbf{e}(t)$ we have

$$\|e^l\|_1^2 \equiv \int_0^1 \left\{ (e^l)^2 + \left(\frac{de^l}{dt} \right)^2 \right\} dt \leqslant \int_0^1 \left(\frac{d^2\theta^l}{dt^2} \right)^2 dt, \qquad l = 1,..., K.$$

Thus, $G(\mathbf{h})$ defined by (1) may be interpreted as an upper bound on a weighted H^1-norm of $\mathbf{e}(t)$ and we anticipate that parametrizations which minimize G will also provide interpolating curves $\boldsymbol{\theta}(t)$ which are closer to the interpolating polygon.

(ii) Other applications for spline interpolation and approximation techniques arise in the design of trajectories to be tracked in time by the axes of robot manipulators [5–7]. Here, when the parameter t is interpreted as a time variable the objective function $G(\mathbf{h})$ gives a weighted measure of average acceleration. Minimizing this measure of average acceleration is consistent with the goal of reducing machine wear.

Prior discussions of parametrization issues appear in [2–5]. References [2–4] deal with geometric applications while [5] treats a robot trajectory problem.

The effects of various parametrizations on the properties of the resulting space curves in parametric cubic spline interpolation problems are considered in [2, 3]. Here the basic conclusion is that the accumulated chord length parametrization is satisfactory for most geometric applications. If d_i, $i = 1,..., N$, denotes the distance between points $\mathbf{z}_{i-1}$ and $\mathbf{z}_i$ then the normalized version of this standard parametrization is given by

$$t_0 = 0, \qquad t_i = t_{i-1} + d_i \Big/ \left(\sum_{j=1}^{N} d_j \right), \quad i = 1,..., N. \tag{5}$$

It is generally found that when two- or three-dimensional data are parametrized according to (5) the resulting parametric cubic spline interpolant has "pleasing" shape. While this subjective assessment is based mainly on experience, results of [2] establish a more concrete reason for using (5). The chord length parametrization does not, however, address the smoothness issue and when used in applications of robot trajectory design, it merely ensures that approximate constant speed is maintained.

The method presented in [4] is a variational approach to a parametrization issue in curve approximation and its intent is to choose a parametrization which allows a given smooth geometric shape to be well approximated by low order piecewise polynomials.

In [5], approximate minimum time trajectories for the axes of a robot manipulator are determined by interpolating appropriately parametrized robot axes data with cubic splines. The parametrization is determined by minimizing total travel time under constraints on the cubic spline velocities, accelerations, and third derivatives.

Our purpose is to consider problem (2) as an approach to the parametrization issue. In Section 2 we examine problem (2) when $K = 1$. Although this case has limited practical application, it is important because it can be solved explicitly and the results provide some insight in the higher dimensional setting. Numerical solution of the problem in higher dimensions is discussed in Section 3. Several sample problems are solved and the results are compared to those obtained using the standard chord length parametrization. Finally, results and conclusions are discussed in Section 4.

2. Solution when $K = 1$

We show in this section that scalar ordinates $z_0, z_1,..., z_N$ satisfying

$$\Delta_i = z_i - z_{i-1} \neq 0, \qquad i = 1,..., N, \tag{6}$$

admit a unique parametrization $0 = t_0^* < t_1^* < \cdots < t_N^* = 1$ (or the equivalent mesh spacing $\mathbf{h}^* = (h_1^*,..., h_N^*)^T$) which minimizes $\int_0^1 (\theta''(t))^2\, dt$, where $\theta(t) \in S_0(t_0^*, t_1^*,..., t_N^*)$, $\theta(t_i^*) = z_i$, $i = 0, 1,..., N$. We consider three cases classified according to the behavior of the sequence of Δ_i's defined in (6) and begin by summarizing the main results in each case.

I. $\Delta_{i+1}/\Delta_i > 0$, $i = 1,..., N-1$

The condition $\Delta_{i+1}/\Delta_i > 0$, $i = 1,..., N-1$, implies that the data $z_0, z_1,..., z_N$ are strictly monotone. In this case the unique minimizing parametrization is the one-dimensional version of normalized accumulated chord length

$$t_0^* = 0, \qquad t_i^* = t_{i-1}^* + |\Delta_i| \Big/ \sum_{j=1}^{N} |\Delta_j|, \qquad i = 1,..., N. \tag{7}$$

With this choice, the interpolating natural cubic spline $\theta(t)$ is a linear polynomial on $[0, 1]$ and $G(\mathbf{h}^*) = \int_0^1 (d^2\theta/dt^2)^2\, dt = 0$.

II. $\Delta_{i+1}/\Delta_i < 0$, $i = 1,..., N-1$

If $\Delta_{i+1}/\Delta_i < 0$, $i = 1,..., N-1$ then each ordinate is either larger or smaller than both of its neighbors (i.e., each ordinate is a relative extreme value). We show in the following lemma that if $0 = t_0^* < \cdots < t_N^* = 1$ is a minimizing parametrization then

$$\frac{d\theta}{dt}(t_i^*) = 0, \qquad i = 1,..., N-1. \tag{8}$$

This uniquely determines $t_0^*, t_1^*,..., t_N^*$ giving the characterization

$$t_0^* = 0, \qquad t_i^* = t_{i-1}^* + \left(\varepsilon_i \sqrt{|\Delta_i|} \Big/ \sum_{j=1}^{N} \varepsilon_j \sqrt{|\Delta_j|}\right), \qquad i = 1,..., N, \tag{9}$$

where $\varepsilon_1 = 1$; $\varepsilon_i = \sqrt{2}$, $i = 2,..., N-1$; $\varepsilon_N = 1$.

LEMMA. *Let* $z_0, z_1,..., z_N \in \mathbb{R}$ *satisfy* $\Delta_{i+1}/\Delta_i < 0$, $i = 1,..., N-1$. *If* $0 = t_0^* < t_1^* < \cdots < t_N^* = 1$ *is a minimizing parametrization for the ordinates* $z_0, z_1,..., z_N$ *then* (8) *holds.*

Proof. If $(d\theta/dt)(t_i^*) \neq 0$ at an interior breakpoint, then there is a point $\hat{t}_i \neq t_i^*$ with $t_{i-1}^* < \hat{t}_i < t_{i+1}^*$ satisfying $\theta(\hat{t}_i) = \theta(t_i^*) = z_i$. This is a conse-

quence of the alternating character of the data and the fact that $(d\theta/dt)(t_i^*) \neq 0$ implies that there is an overshoot in a neighborhood of t_i^*. Next let $\psi(t) \in S_0(t_0^*,..., t_{i-1}^*, \hat{t}_i, t_{i+1}^*,..., t_N^*)$ satisfy $\psi(t_j^*) = z_j$, $j \neq i$, $\psi(\hat{t}_i) = z_i$. Since $\theta(t)$ interpolates $\{z_i\}_{i=0}^{N}$ at the same abscissa, the minimum properties of $\psi(t)$ from [8] require that

$$\int_0^1 \left(\frac{d^2\psi}{dt^2}\right)^2 dt \leqslant \int_0^1 \left(\frac{d^2\theta}{dt^2}\right)^2 dt.$$

But $t_0^*,..., t_i^*,..., t_N^*$ is a minimizing parametrization for the ordinates $z_0, z_1,..., z_N$ so the reverse inequality must hold as well. Hence, from [8], $\theta(t) \equiv \psi(t)$, $t \in [0, 1]$. By comparing the breakpoints of the natural cubic splines θ and ψ, we conclude that if $(d\theta/dt)(t_i^*) \neq 0$ at an interior parameter value t_i^* then $\theta(t)$ is a cubic polynomial in the interval $[t_{i-1}^*, t_{i-1}^*]$. We can repeat the above argument and enlarge the interval $[t_{i-1}^*, t_{i-1}^*]$ to $[t_A, t_B]$, where $t_A = t_0^*$ or $(d\theta/dt)(t_A) = 0$ and $t_B = t_N^*$ or $(d\theta/dt)(t_B) = 0$. In any case we have that $\theta(t)$ is a cubic polynomial on $[t_A, t_B]$ which, because of the alternating data, has at least one interior extreme value and satisfies $(d^2\theta/dt^2)(t_A) = 0$ or $(d\theta/dt)(t_A) = 0$ and $(d^2\theta/dt^2)(t_B) = 0$ or $(d\theta/dt)(t_B) = 0$. This requires that $\theta \equiv$ constant on $[t_A, t_B]$, a contradiction in view of its interpolation properties.

Uniqueness and the characterization (9) are established as follows.

COROLLARY 1. *The unique minimizing parametrization for ordinates* $z_0, z_1,..., z_N$ *satisfying* $\Delta_{i+1}/\Delta_i < 0$, $i = 1,..., N-1$ *is given by* (9).

Proof. We show (9) is the only parametrization $0 = t_0 < t_1 < \cdots < t_N = 1$ of the ordinates for which the interpolating natural cubic spline $\theta(t) \in S_0(t_0, t_1,..., t_N)$, in addition to having two continuous derivatives and satisfying

$$(d^2\theta/dt^2)(t_0) = (d^2\theta/dt^2)(t_N) = 0, \quad \theta(t_i) = z_i, \quad i = 0, 1,..., N, \text{ also satisfies } (d\theta/dt)(t_i) = 0, \; i = 1,..., N-1. \tag{10}$$

It then follows from existence and the lemma that this must be the minimizing parametrization.

At each breakpoint t_i, $i = 0,..., N$, we know the value of $\theta(t_i)$ and either $(d\theta/dt)(t_i)$ or $(d^2\theta/dt^2)(t_i)$. This allows the piecewise cubic $\theta(t)$ to be reconstructed locally using Hermite cubics. In doing so we find, in general, that there is a jump in the second derivative at interior breakpoints given by

$$\frac{d^2\theta}{dt^2}(t_i^+) - \frac{d^2\theta}{dt^2}(t_i^-) = \left(\frac{3\varepsilon_{i+1}^2\Delta_{i+1}}{h_{i+1}^2}\right) - \left(-\frac{3\varepsilon_i^2\Delta_i}{h_i^2}\right), \quad i = 1,..., N-1, \tag{11}$$

where $h_i = t_i - t_{i-1}$, $i = 1,..., N$, and $\varepsilon_i, i = 1,..., N$, are as defined in (9). Since $\theta(t)$ has continuous second derivatives, the right-hand side of (11) must vanish. This yields

$$\left(\frac{h_{i+1}}{h_i}\right)^2 = \frac{\varepsilon_{i+1}^2 \Delta_{i+1}}{-\varepsilon_i^2 \Delta_i} = \frac{\varepsilon_{i+1}^2}{\varepsilon_i^2} \left|\frac{\Delta_{i+1}}{\Delta_i}\right|, \qquad i = 1,..., N-1. \tag{12}$$

Under the additional condition $\sum_{i=1}^{N} h_i = 1$, the Eqs. (12) are uniquely solvable and provide

$$h_i = \varepsilon_i \sqrt{|\Delta_i|} \Big/ \sum_{j=1}^{N} \varepsilon_j \sqrt{|\Delta_j|}, \qquad i = 1,..., N.$$

This mesh spacing induces the parametrization given in (9).

III. *Δ_{i+1}/Δ_i Changes Sign*

In this general case we first identify all indices $1 \leqslant i_1 < \cdots < i_{M-1} \leqslant N-1$ for which $\Delta_{i_k+1}/\Delta_{i_k} < 0$, let $i_0 = 0$, $i_M = N$ and define

$$D_{i_k} = z_{i_k} - z_{i_{k-1}}, \qquad k = 1,..., M. \tag{13}$$

The edited data $z_{i_0}, z_{i_1},..., z_{i_M}$ are governed by case II ($D_{i_{k+1}}/D_{i_k} < 0$, $k = 1,..., M-1$) and has a unique minimizing parametrization

$$0 = \hat{t}_{i_0} < \hat{t}_{i_1} < \cdots < \hat{t}_{i_M} = 1. \tag{14}$$

This parametrization can be refined in a natural way to generate a complete parametrization $t_0^*, t_1^*,..., t_N^*$ of the original ordinates. To accomplish this let

$$\psi(t) \in S_0(\hat{t}_{i_0}, \hat{t}_{i_1},..., \hat{t}_{i_M}) \qquad \text{with} \qquad \psi(\hat{t}_{i_k}) = z_{i_k}, \quad k = 0,..., M. \tag{15}$$

For an index $j \in \{0, 1,..., N\}$, define the parameter value t_j^* as follows. When $j = i_k$ for some $k \in \{0, 1,..., M\}$ simply set

$$t_j^* = \hat{t}_{i_k}. \tag{16}$$

If $i_{k-1} < j < i_k$ for some $k \in \{1,..., M\}$ then define t_j^* as the solution in $[\hat{t}_{i_{k-1}}, \hat{t}_{i_k}]$ of the equation

$$\psi(t_j^*) = z_j. \tag{17}$$

The validity of the definitions (16) and (17) follows from two additional observations.

(i) If $i_{k-1} < j < i_k$, then z_j is in the open interval spanned by $z_{i_{k-1}}$ and z_{i_k} and

(ii) $\psi(\hat{t}_{i_k}) = z_{i_k}$, $k = 0, 1, \ldots, M$, and $\psi(t)$ is strictly monotone (a consequence of (8)) on the interval $[\hat{t}_{i_{k-1}}, \hat{t}_{i_k}]$.

Observations (i) and (ii) guarantee that Eq. (17) is uniquely solvable and that the resulting set of parameter values $\{t_i^*\}_{i=0}^N$ satisfies $0 = t_0^* < t_1^* < \cdots < t_N^* = 1$. Additional arguments, given in Corollary 2, establish this as the unique minimizing parametrization for $z_0, z_1, \ldots, z_N$.

COROLLARY 2. *The parametrization* $0 = t_0^* < t_1^* < \cdots < t_N^* = 1$ *defined by* (16) *and* (17) *is the unique minimizing parametrization for* $z_0, z_1, \ldots, z_N$.

Proof. Let $0 = \tilde{t}_0 < \tilde{t}_1 < \cdots < \tilde{t}_N = 1$ be any minimizing parametrization for $z_0, z_1, \ldots, z_N$ and define

$$\tilde{\theta}(t) \in S_0(\tilde{t}_0, \tilde{t}_1, \ldots, \tilde{t}_N), \qquad \tilde{\theta}(\tilde{t}_i) = z_i, \quad i = 0, \ldots, N. \tag{18}$$

We will show that $\tilde{t}_i = t_i^*$, $i = 0, \ldots, N$. To begin we let

$$\theta(t) \in S_0(t_0^*, t_1^*, \ldots, t_N^*), \qquad \theta(t_i^*) = z_i, \quad i = 0, \ldots, N. \tag{19}$$

Then by the construction of $t_0^*, t_1^*, \ldots, t_N^*$ we must have that

$$\theta(t) \equiv \psi(t), \qquad t \in [0, 1], \tag{20}$$

where $\psi(t) \in S_0(\hat{t}_{i_0}, \hat{t}_{i_1}, \ldots, \hat{t}_{i_M})$ is given by (15). With the subsequence of indices, i_k, $k = 0, 1, \ldots, M$, defined as before, let

$$\tilde{\psi}(t) \in S_0(\tilde{t}_{i_0}, \tilde{t}_{i_1}, \ldots, \tilde{t}_{i_M}), \qquad \tilde{\psi}(\tilde{t}_{i_k}) = z_{i_k}, \quad k = 0, \ldots, M.$$

The minimum property of $\hat{t}_{i_0}, \hat{t}_{i_1}, \ldots, \hat{t}_{i_M}$ introduced just prior to Eq. (14) (note that $\hat{t}_{i_k} = t_{i_k}^*$, $k = 0, 1, \ldots, M$) gives

$$\int_0^1 \left(\frac{d^2\psi}{dt^2}\right)^2 dt \leqslant \int_0^1 \left(\frac{d^2\tilde{\psi}}{dt^2}\right)^2 dt. \tag{21}$$

The minimum property of the $\tilde{\psi}(t)$ from [8] yields

$$\int_0^1 \left(\frac{d^2\tilde{\psi}}{dt^2}\right)^2 dt \leqslant \int_0^1 \left(\frac{d^2\tilde{\theta}}{dt^2}\right)^2 dt. \tag{22}$$

Since $\tilde{t}_0, \tilde{t}_1, \ldots, \tilde{t}_N$ is a minimizing parametrization of $z_0, z_1, \ldots, z_N$, we also have

$$\int_0^1 \left(\frac{d^2\tilde{\theta}}{dt^2}\right)^2 dt \leqslant \int_0^1 \left(\frac{d^2\theta}{dt^2}\right)^2 dt. \tag{23}$$

Inequalities (21)–(23) and Eq. (20) combine to yield

$$\int_0^1 \left(\frac{d^2\tilde{\theta}}{dt^2}\right)^2 dt = \int_0^1 \left(\frac{d^2\theta}{dt^2}\right)^2 dt \tag{24}$$

and

$$\int_0^1 \left(\frac{d^2\tilde{\psi}}{dt^2}\right)^2 dt = \int_0^1 \left(\frac{d^2\psi}{dt^2}\right)^2 dt. \tag{25}$$

Equation (24) shows that $t_0^*, t_1^*,..., t_N^*$ is a minimizing parametrization for $z_0, z_1,..., z_N$ while Eq. (25), together with case II uniqueness implies uniqueness in this case. The immediate implication of (25) and case II uniqueness is that

$$\hat{t}_{i_k} = t_{i_k}^*, \qquad k = 0, 1,..., M,$$

and (26)

$$\tilde{\psi}(t) = \psi(t), \qquad t \in [0, 1].$$

From (20) we obtain

$$\tilde{\psi}(t) = \theta(t), \qquad t \in [0, 1]. \tag{27}$$

Thus, (24) now gives

$$\int_0^1 \left(\frac{d^2\tilde{\theta}}{dt^2}\right)^2 dt = \int_0^1 \left(\frac{d^2\tilde{\psi}}{dt^2}\right)^2 dt. \tag{28}$$

The minimum property of $\tilde{\psi}(t)$ from [8] states that Eq. (28) can hold only when

$$\tilde{\psi}(t) \equiv \tilde{\theta}(t), \qquad t \in [0, 1]. \tag{29}$$

Equations (26), (27), and (29) imply finally that

$$\tilde{t}_i = t_i^*, \qquad i = 0, 1,..., N.$$

The preceding results and discussion also establish several noteworthy properties of the interpolating natural cubic spline associated with the minimizing parametrization of scalar ordinates. These are summarized.

COROLLARY 3. *Let* $\theta(t) \in S_0(t_0^*, t_1^*,..., t_N^*)$ *satisfy* $\theta(t_i^*) = z_i$, $i = 0, 1,..., N$, *where* $t_0^*, t_1^*,..., t_N^*$ *is the minimizing parametrization for ordinates* $z_0, z_1,..., z_N$ *satisfying* (6). *Then*

(i) *$\theta(t)$ interpolates the data (t_i^*, z_i), $i = 0, 1, \ldots, N$, with no overshoots.*

(ii) *$\theta(t) \in S_0(t_{i_0}^*, t_{i_1}^*, \ldots, t_{i_M}^*)$, where $0 = i_0 < i_1 < \cdots < i_M = N$ is the list of indices which locate endpoints and interior relative extreme values of the ordinates.*

(iii) $\theta''(t_{i_k}) = -3\ \mathrm{sgn}(D_{i_k})(\sum_{j=1}^{M} \varepsilon_j \sqrt{|D_j|})^2$, $k = 1, 2, \ldots, M-1$, *where*

$$\begin{aligned} D_{i_k} &= z_{i_k} - z_{i_{k-1}}, && k = 1, \ldots, M, \\ \varepsilon_j &= 1 && \text{if } j = 1 \text{ or } M, \\ &= \sqrt{2} && \text{if } j = 2, \ldots, M-1, \end{aligned}$$

and

$$\begin{aligned} \mathrm{sgn}(D_{i_k}) &= +1 && \text{if } D_{i_k} > 0, \\ &= -1 && \text{if } D_{i_k} < 0. \end{aligned}$$

Consequences of properties (i) and (ii) in the interpolation of scalar data are the elimination of position overshoots and the reduction of the number of essential breakpoints in the spline representation. The third property highlights a somewhat special behavior in the second derivative. The peak second derivatives, which occur at interior breakpoints, alternate in sign but remain constant in magnitude. These points are further illustrated by Fig. 1. Here we show the interpolating natural cubic spline, together with its first and second derivatives, for the data $\{(t_i^*, z_i)\}_{i=0}^{10}$ given in Table 1.

When higher dimensional data is parametrized by solving (2), the associated natural cubic spline interpolants of the data components do not satisfy precisely the properties listed in Corollary 3. However, by comparing numerical results using the parametrization (5) with results obtained using a solution of (2) we generally find that:

(i) Position overshoots are reduced.

(ii) The jump in the 3rd derivative is reduced at breakpoints not coinciding with relative extreme values.

(iii) Oscillations in the second derivative tend to be more centered about zero.

These points will be illustrated by examples in Section 3.

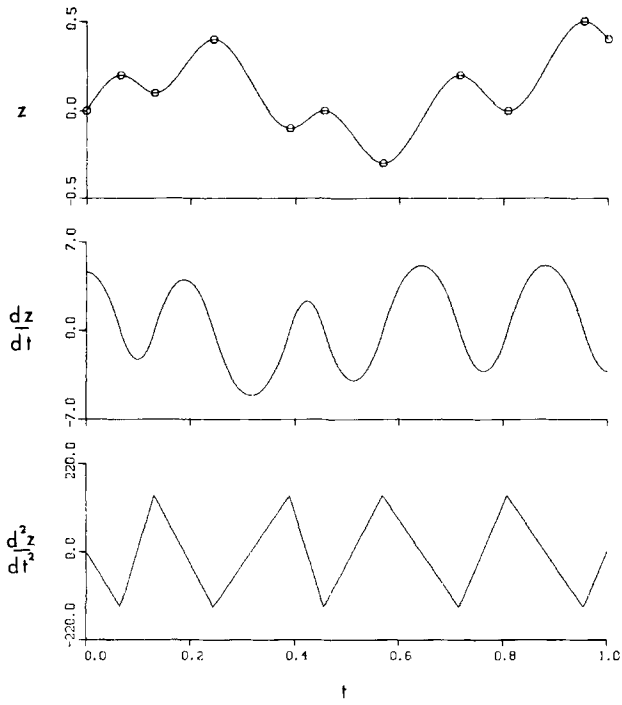

FIG. 1. Cubic spline fit of the data from Table I using minimizing parametrization.

TABLE I

Sample One-Dimensional Data

i	z_i	t_i^*
0	0.0	0.0
1	0.2	0.0654
2	0.1	0.1308
3	0.4	0.2440
4	−0.1	0.3902
5	0.0	0.4556
6	−0.3	0.5689
7	0.2	0.7151
8	0.0	0.8076
9	0.5	0.9538
10	0.4	1.0000

Note. The ordinates $\{z_i\}_{i=0}^{10}$ and the minimizing parameterization $\{t_i^*\}_{i=0}^{10}$.

3. Higher Dimensional Problems—Numerical Experiments

The results and discussion of Section 2 are specific to the case $K = 1$ and do not carry over to the higher dimensional problems. We can, however, treat problem (2) numerically with $K > 1$ and show that good parametrizations can be obtained by attempting to minimize $G(\mathbf{h})$ within the constraint set (3).

Numerical results are obtained using a gradient projection method [9] to find local minima. We briefly outline this approach. Starting with an initial parametrization $\mathbf{h}^{(0)} \in B = \{\mathbf{h} \mid h_i \geqslant 0,\ \sum_{i=1}^{N} h_i = 1\}$ a sequence $\mathbf{h}^{(1)}$, $\mathbf{h}^{(2)}$,..., of iterates in B is generated according to

$$\mathbf{h}^{(i)} = \mathbf{h}^{(i-1)} - \lambda^{(i-1)} \pi_B(\nabla G\,|_{\mathbf{h}^{(i-1)}}). \tag{30}$$

In (30) $\nabla G = (\partial G/\partial h_1,..., \partial G/\partial h_N)^{\mathrm{T}}$ and π_B is the projection of R^N onto the subspace $\{\mathbf{x} \in R^N \mid \mathbf{x} \cdot \hat{n} = 0\}$, where $\hat{n} = (1/\sqrt{N})(1, 1,..., 1)^{\mathrm{T}} \in R^N$. In particular,

$$\pi_B(\mathbf{y}) = \mathbf{y} - (\mathbf{y} \cdot \hat{n})\hat{n}.$$

The parameter $\lambda^{(i-1)}$ is the nonnegative scalar quantity which solves the one-dimensional problem

$$\underset{\lambda \in [0, \lambda_{\max}]}{\text{minimize}}\ f(\lambda) = G(\mathbf{h}^{(i-1)} - \lambda \pi_B(\nabla G\,|_{\mathbf{h}^{(i-1)}})),$$

where $\lambda_{\max}$ is the largest λ for which $\mathbf{h}^{(i-1)} - \lambda \pi_B(\nabla G\,|_{\mathbf{h}^{(i-1)}})$ has nonnegative components. This method results in a sequence of parametrizations $\mathbf{h}^{(0)}$, $\mathbf{h}^{(1)}$,..., for which the corresponding sequence of objective values $G(\mathbf{h}^{(0)})$, $G(\mathbf{h}^{(1)})$,..., $G(\mathbf{h}^{(l)})$,..., is nonincreasing. Thus if we choose the parametrization (5) to define the initial guess $\mathbf{h}^{(0)}$, the procedure outlined above will always result in an improved parametrization, according to our criterion, provided $\pi_B(\nabla G\,|_{\mathbf{h}^{(0)}}) \neq \mathbf{0}$.

Calculations are carried out by expressing $G(\mathbf{h})$ in algebraic form. Using notation introduced in Section 1, we can write

$$G(\mathbf{h}) = \sum_{l=1}^{K} \frac{1}{\alpha_l^2} (\mathbf{z}^l)^{\mathrm{T}}\, Q^{\mathrm{T}}(\mathbf{h})\, M^{-1}(\mathbf{h})\, Q(h)\, \mathbf{z}^l. \tag{31}$$

Here $\mathbf{z}^l = (z_0^l, z_1^l,..., z_N^l)^{\mathrm{T}}$, $Q = (Q_{ij})^{i=1,\ldots,N-1,\, j=0,\ldots,N}$, and $M = (M_{ij})_{i,j=1,\ldots,N-1}$ with the matrices Q and M defined by

$$
\begin{aligned}
Q_{ij} &= 1/h_i, && j = i-1, \\
&= -(1/h_{i+1} + 1/h_i), && j = i, \\
&= 1/h_{i+1}, && j = i+1, \\
&= 0, && \text{otherwise;}
\end{aligned}
\qquad
\begin{aligned}
M_{ij} &= h_i/6, && j = i-1, \\
&= (h_i + h_{i+1})/3, && j = i, \\
&= h_{i+1}/6, && j = i+1, \\
&= 0, && \text{otherwise.}
\end{aligned}
$$

The representations (31) follows from standard smoothest interpolation results from natural cubic spline interpolation (see [1]).

The weights α_l, $l = 1,..., K$, for geometric applications are choosen according to

$$\alpha_l = 1, \qquad l = 1,..., K, \tag{32}$$

while for problems in trajectory design they are selected according to the acceleration capabilities of the robot's axes, for example,

$$\alpha_l = \text{acceleration limit for the } l\text{th axis.} \tag{33}$$

This strategy is adhered to in the accompanying examples and has been effective in establishing the appropriate hierarchy among the terms of (31). We note, however, that (32) may not be appropriate in geometric examples when the data are poorly scaled.

A modification to (31) which simplifies computation and does not appear to detract from the effectiveness of the procedure can be obtained by replacing M by the matrix $\hat{M}$ consisting merely of the diagonal terms of M, that is, $\hat{M}_{ij} = 0$, $i \neq j$, $\hat{M}_{ii} = M_{ii}$. This change has the same effect as replacing the integrals in (1) by rectangular quadratures with mesh spacing $\mathbf{h}$ and then substituting centered difference approximations for the second derivatives at mesh points. The resulting objective function

$$G(\mathbf{h}) = \sum_{l=1}^{K} \frac{1}{\alpha_l^2} (\mathbf{z}^l)^{\mathrm{T}} Q^{\mathrm{T}}(\mathbf{h}) \hat{M}^{-1}(\mathbf{h}) Q(\mathbf{h}) \mathbf{z}^l \tag{34}$$

reduces the computational burden by eliminating the necessity of solving a tridiagonal system when evaluating G.

We consider three examples to illustrate the method. The first two are two-dimensional curve fitting problems and the third is a problem in trajectory design for a six axes robot manipulator.

In the first example we fit a curve to the plane data $\{(x_i, y_i)\}_{i=0}^{19}$ given in Table II. The initial parametrization is normalized accumulated chord length and is denoted by t_i^{CL}. The gradient projection method was applied to (2), first with G defined exactly by (31) to generate $t_i^{\mathrm{EX}} i = 0,..., 19$ and then with G defined approximately by (34) to generate the parametrization $t_i^{\mathrm{AP}} i = 0,..., 19$. These parametrizations are listed in Table III. The resulting

TABLE II

Sample Data $\{(x_i, y_i)\}_{i=0}^{19}$ for Two-Dimensional Curve Fitting Problem

i	x_i	y_i
0	0.530	0.720
1	0.470	0.750
2	0.365	0.760
3	0.260	0.735
4	0.205	0.695
5	0.200	0.660
6	0.235	0.590
7	0.340	0.520
8	0.475	0.445
9	0.550	0.350
10	0.565	0.300
11	0.550	0.240
12	0.500	0.200
13	0.420	0.180
14	0.310	0.180
15	0.220	0.200
16	0.150	0.230
17	0.105	0.275
18	0.080	0.340
19	0.090	0.385

TABLE III

Parametrizations of the Data from Table II

i	$t_i^{(1)}$	$t_i^{(2)}$	$t_i^{(3)}$
0	0.0	0.0	0.0
1	0.0424	0.0365	0.0363
2	0.1091	0.0961	0.0952
3	0.1773	0.1617	0.1616
4	0.2203	0.2192	0.2187
5	0.2426	0.2538	0.2535
6	0.2921	0.3146	0.3139
7	0.3719	0.3859	0.3847
8	0.4695	0.4641	0.4624
9	0.5460	0.5347	0.5322
10	0.5790	0.5712	0.5697
11	0.6181	0.6214	0.6200
12	0.6586	0.6689	0.6680
13	0.7107	0.7183	0.7184
14	0.7802	0.7760	0.7767
15	0.8385	0.8239	0.8255
16	0.8866	0.8678	0.8699
17	0.9268	0.9099	0.9123
18	0.9709	0.9636	0.9646
19	1.0000	1.0000	1.0000

Note. $\{t^{(1)}\}_{i=0}^{19}$ is normalized accumulated chord length; $\{t_i^{(2)}\}_{i=0}^{19}$ and $\{t^{(3)}\}_{i=0}^{19}$ are the minimizing parametrizations corresponding to objective functions (31) and (34), respectively.

plane curves, generated by interpolating the component data with natural cubic splines and plotting the resulting parametric curves, are nearly identifical for the three parametrizations. The curve corresponding to the parametrization $\{t_i^{EX}\}_{i=0}^{19}$ is shown in Fig. 2. Here the open dots locate the data from Table II. More pronounced differences are evident when we look at component functions. In Figs. 3–5 we plot the natural cubic splines $x(t)$, $y(t)$ vs t for each of the three parametrizations along with their first and second derivatives. Comparison of the results in Fig. 3 with those of Fig. 4 or Fig. 5 reveals substantial reduction in the second derivatives for both component functions, indicative of the expected improvements in smoothness. The validity of using the approximate objective function (34) in place of the exact one (31) is also illustrated by comparing Figs. 4 and 5. Regarding the three comments made at the end of Section 2 we note first that position overshoots are not a problem in any of the parametrizations of this data. Smaller jumps in third derivatives are evident, however, and oscillations in the second derivative are more centered about zero. These observations are most pronounced when the plot of d^2x/dt^2 vs t from Fig. 3 is compared to the one in Fig. 4.

In our second example we illustrate the conformity issue discussed in (i), Section 1. For this example we consider the data (open dots) and the interpolating polygon (solid curve) shown in Fig. 6. When these data are parametrized by (5) and the components interpolated with natural cubic

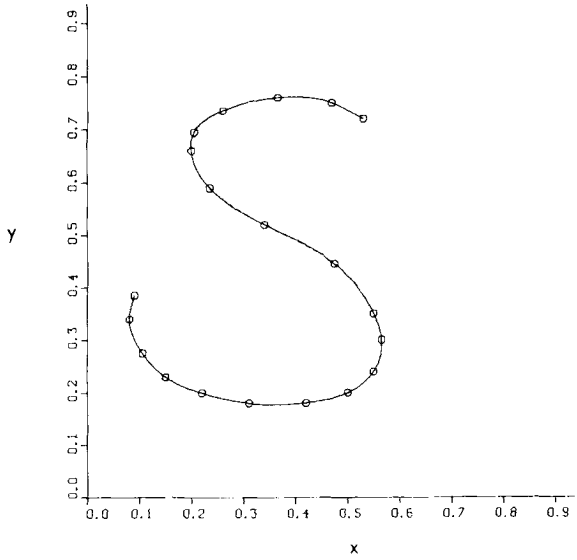

FIG. 2. Parametric cubic spline fit of the two dimensional data from Table II. The curve shown corresponds to the minimizing parametrization $\{t_i^{EX}\}_{i=0}^{19}$.

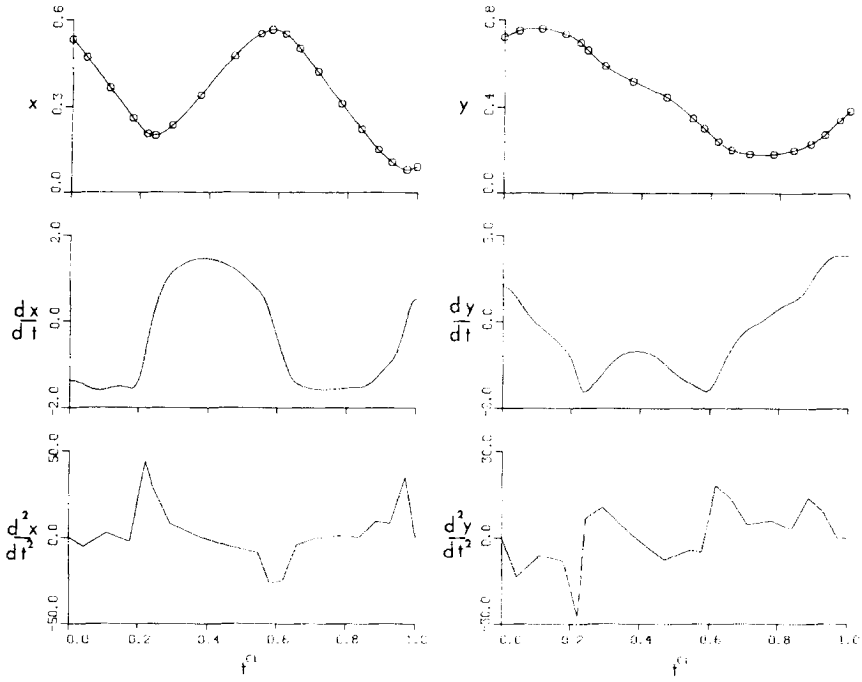

FIG. 3. Plots of position, first and second derivatives for each component of the parametric cubic spline fit of the data from Table II. The parametrization used is normalized accumulated chord length.

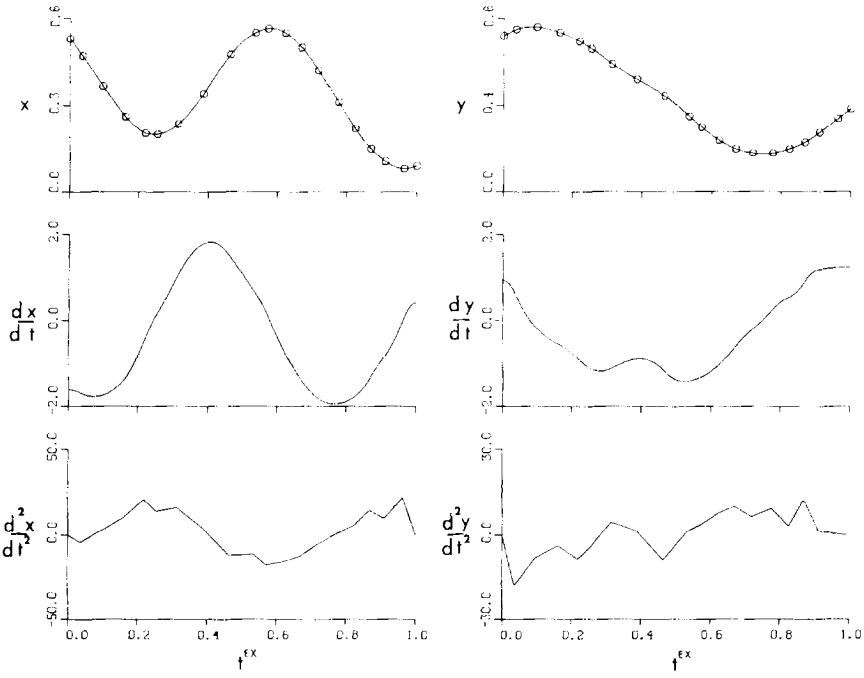

FIG. 4. Plots of position, first and second derivatives for each component of the parametric cubic spline fit of the data from Table II. The parametrization is t^{EX}, the minimizing parametrization based on the objective function (31).

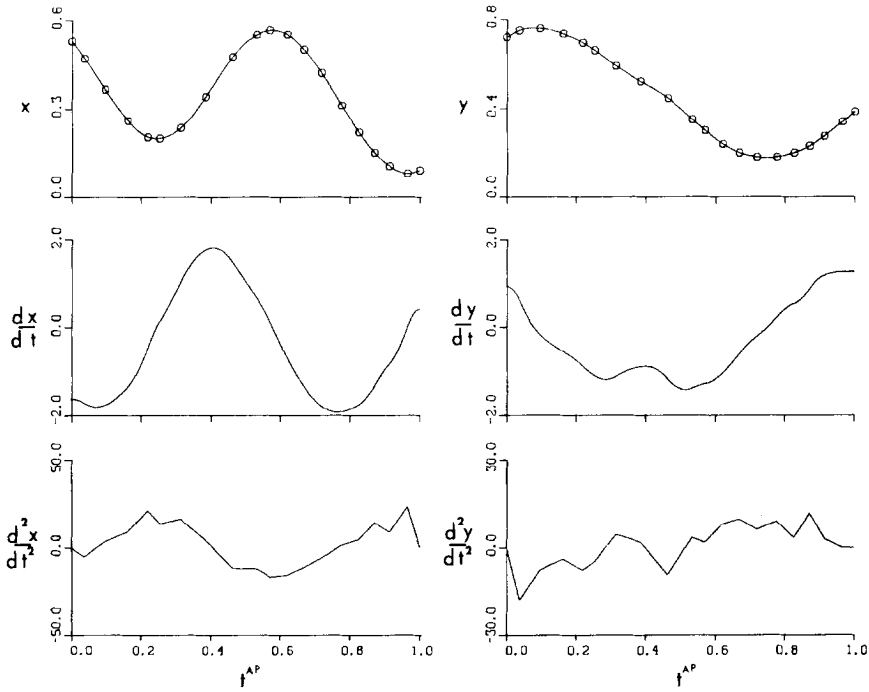

FIG. 5. Plots of position, first and second derivatives for each component of the parametric cubic spline fit of the data from Table II. The parametrization used is t^{AP}, the minimizing parametrization based on objective function (34).

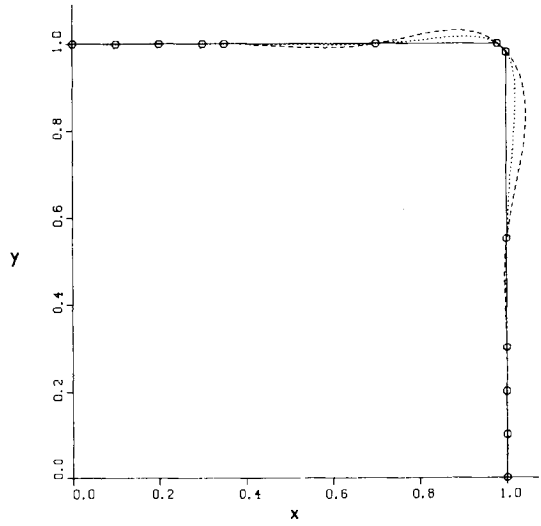

FIG. 6. Interpolation of planar data. The solid curve is the piecewise linear interpolant, the dashed curve is the parametric cubic spline interpolant obtained using normalized accumulated chord length (5), and the dotted curve is the parametric cubic spline interpolant corresponding to the minimizing parametrization.

splines the resulting smooth curve undergoes several oscillations near the corner (dashed curve, Fig. 6). The amplitude of these oscillations can be reduced by choosing the parametrization according to the minimization problem (2). The dotted curve in Fig. 6 is the parametric curve obtained by parametrizing the data with the minimizing parametrization and interpolating with the natural cubic splines. The behavior noted here was observed in a number of examples and appears to be most pronounced when the data are widely spaced near corners.

Our third example illustrates the method applied to data from a six axes robot manipulator. A diagram of the manipulator is shown in Fig. 7. As the manipulator's joints assume the required positions, displayed in Table IV, the work center, of the machine denoted P in Fig. 7, will pass through particular points (x, y, z) in space. These points are listed in Table V and provide a convenient geometric interpretation for these six-dimensional data. The relative acceleration limits α_l, $l = 1,\ldots, 6$, used in (31) or (34) are $\alpha_1 = \alpha_2 = 1$, $\alpha_3 = 2$, $\alpha_4 = \alpha_5 = \alpha_6 = 6$. For this example we use only the approximate objective function defined by (34) to generate the minimizing parametrization $\{t_i^{AP}\}_{i=0}^{20}$. We compare these results with two standard parametrizations of the manipulator data. The first of these is normalized accumulated chord length $\{t_i^{CL}\}_{i=0}^{20}$ based on the six-dimensional data and the second is normalized accumulated chord length $\{t_i^{WC}\}_{i=0}^{20}$ based on the associated three-dimensional data, the work center positions. We remark that the second parametrization is not always valid because distinct manipulator axis positions do not always give rise to distinct work center positions. The three parametrizations are given in Table VI. Results obtained after interpolating the component data with natural cubic splines for each of the three parametrizations are shown in Figs. 8, 9 and Table VII. Figs. 8a–8c give the xz projections of the smooth path followed by the work center position of the manipulator for each of the three parametrizations. Table VII is a list of the

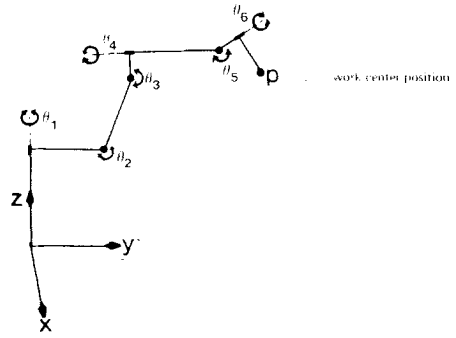

FIG. 7. Diagram of the six axes robot manipulator.

TABLE IV

Sample Data from the Six Axes Robot Manipulator Shown in Fig. 7

i	θ_i^1(RAD)	θ_i^2(RAD)	θ_i^3(RAD)	θ_i^4(RAD)	θ_i^5(RAD)	θ_i^6(RAD)
0	0.0072	0.2117	−1.9315	0.3886	1.5031	−0.2466
1	0.2813	0.2136	−1.8714	−0.4775	1.4120	0.5327
2	0.5135	0.1956	−1.7885	−0.9205	1.2095	1.2631
3	0.5192	0.2650	−1.7594	−0.4811	0.5829	2.4066
4	0.5047	0.2510	−1.7515	−0.3523	0.5021	3.0694
5	0.2879	0.2937	−1.8590	−0.0791	0.4807	3.0074
6	−0.0048	0.3259	−1.9315	−0.2773	0.4353	2.7167
7	−0.3815	0.2901	−1.8290	0.5207	0.4178	3.0394
8	−0.5212	0.2591	−1.7542	0.7683	0.4773	3.5202
9	−0.5302	0.2585	−1.7350	0.6651	0.4766	3.5202
10	−0.6377	0.2992	−1.7422	0.4139	0.2934	2.0606
11	−0.7280	0.3043	−1.6963	0.0202	0.4179	1.5481
12	−0.6924	0.2914	−1.5487	0.3629	1.2309	1.1987
13	−0.7009	0.5287	−1.6963	0.6735	1.2663	1.6121
14	−0.6826	0.7766	−1.8351	0.7470	1.2266	1.5462
15	−0.5877	0.9718	−1.8897	0.8447	0.9359	1.5690
16	−0.4669	1.1200	−1.9080	1.0760	0.7418	1.7231
17	−0.4237	1.1686	−1.8934	0.9913	0.7681	1.6836
18	−0.3810	1.0814	−1.7874	0.3615	0.7976	1.0593
19	−0.3677	0.9236	−1.5804	0.1701	0.7789	0.9752
20	−0.3221	0.8646	−1.4953	−0.2526	0.9583	0.5649

TABLE V

Work Center Positions Corresponding to the Manipulator Data Given in Table IV

i	x	y	z
0	0.1228	1.1221	0.1621
1	−0.5478	1.1588	0.1926
2	−0.8349	0.8909	0.3306
3	−1.1100	1.1270	0.5510
4	−1.0043	1.5142	0.5633
5	−0.5581	1.6352	0.5586
6	−0.2105	1.5871	0.5432
7	0.7887	1.5591	0.5460
8	1.1029	1.2715	0.5420
9	1.1287	1.3234	0.5523
10	0.9630	1.5983	0.5130
11	0.9145	1.5002	0.4751
12	1.1597	1.7580	0.5920
13	1.3047	1.7606	1.0331
14	1.2925	1.7792	1.3120
15	1.1510	1.9127	1.5705
16	0.9987	2.0052	1.8403
17	0.8820	2.0689	1.9480
18	0.6165	2.2152	1.6824
19	0.6288	2.3520	1.6123
20	0.6335	2.4119	1.5021

TABLE VI

Parametrizations of the Data from Table IV

i	t_i^{CL}	t_i^{WC}	t_i^{AP}
0	0.0	0.0	0.0
1	0.0897	0.0934	0.0472
2	0.1578	0.1510	0.0996
3	0.2607	0.2219	0.1627
4	0.3115	0.2583	0.2020
5	0.3393	0.3223	0.2604
6	0.3742	0.3710	0.3141
7	0.4448	0.5094	0.3850
8	0.4872	0.5684	0.4374
9	0.4950	0.5765	0.4527
10	0.6068	0.6213	0.5267
11	0.6565	0.6373	0.5694
12	0.7283	0.6892	0.6392
13	0.7722	0.7535	0.6995
14	0.7949	0.7922	0.7457
15	0.8233	0.8370	0.7865
16	0.8524	0.8818	0.8309
17	0.8612	0.9055	0.8561
18	0.9283	0.9612	0.9176
19	0.9533	0.9826	0.9678
20	1.0000	1.0000	1.0000

Note. $\{t_i^{CL}\}_{i=0}^{20}$ is normalized accumulated chord length based on the six dimensional data from Table IV; $\{t_i^{WC}\}_{i=0}^{20}$ is normalized accumulated chord length based on the work center positions in Table V; and $\{t_i^{AP}\}_{i=0}^{20}$ is the minimizing parametrization corresponding to the objective function (34).

TABLE VII

Maximum Acceleration Along Each Cubic Spline Axis Trajectory for the Various Parametrizations[a]

j	1	2	3	4	5	6
t^{CL}	310	280	330	1700	730	890
t^{WC}	350	380	480	1700	920	2100
t^{AP}	120	100	120	470	370	820

[a] $\max_{t\in[0,1]} \left| \frac{d^2\theta^j}{dt^2}(t) \right|, j = 1,\ldots, 6.$

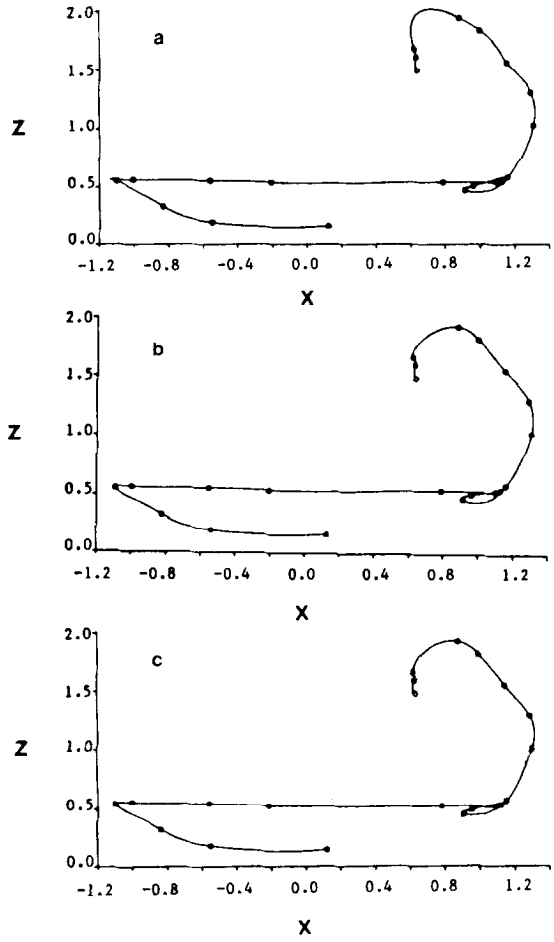

FIG. 8. Projection xz of the path followed by the work center position for the various parametrizations: (a) normalized accumulated chord length based on the six-dimensional axis data; (b) normalized accumulated chord length based on the three-dimensional work center position data; (c) minimizing parametrization.

maximum second derivatives, $\max_{t\in[0,1]} |(d^2\theta^j/dt^2)(t)|$, $j = 1,..., 6$, for each parametrization and Figs. 9a–c are plots of the natural cubic spline interpolants of the axis #3 data for each of the three parametrizations. In this example we do observe some differences among the geometric paths shown in Figs. 8a–c. The major differences do, as in example 1, occur at the component function level. Based on the results shown in Table VII, the minimizing parametrization can reduce significantly component function accelerations compared to those obtained with the other two

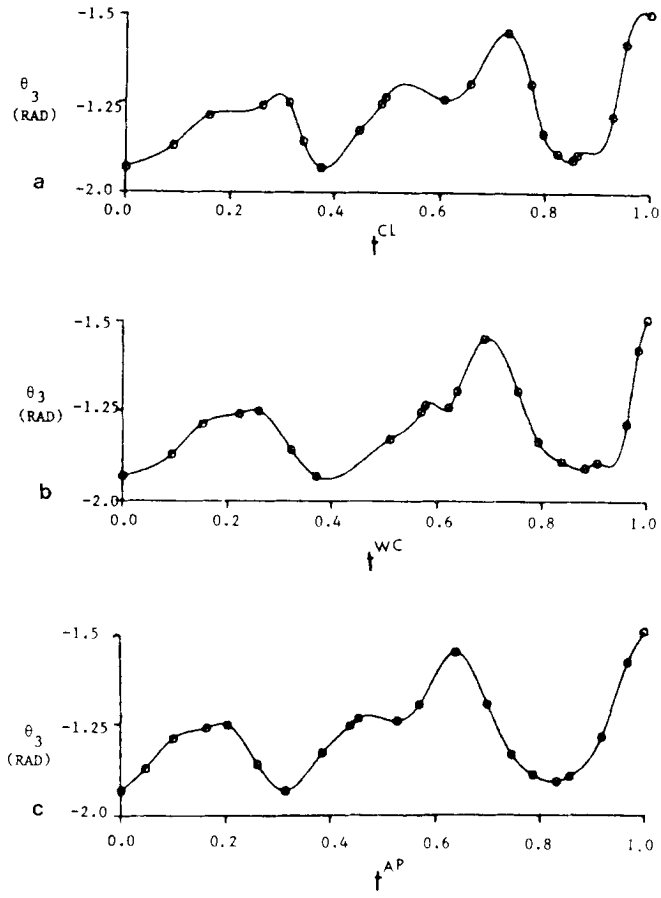

FIG. 9. Cubic spline fit to axis #3 data for each of the parametrizations.

parametrizations. Reduction by a factor of two or more was obtained on five of the six axes. In the case of a mechanical manipulator with dynamic limitations this could mean the difference between being able to complete a task within a required time period or being forced to redefine or eliminate the task. A closer inspection of individual axis motions also reveals that, as in the one-dimensional case, the minimizing parametrization tends to align local extrema in the data with local extrema in the cubic spline interpolant of the data. To illustrate this we consider Figs. 9a–9c, where the natural cubic spline interpolant for axis #3 position is plotted as a function of normalized time for each of the three parametrizations. In the first two cases, Figs. 9a, b, overshoots or unwanted oscillations occur in several areas. These are

eliminated in Fig. 9c, where the results plotted correspond to the minimizing parametrizations $\{t_i^{AP}\}_{i=0}^{20}$.

4. Summary

By basing the choice of parametrization on the certain properties of the component functions we have introduced a fixed, well-defined objective to be met in choosing the parametrizations. This is in contrast with somewhat subjective criteria frequently used to evaluate parametrizations in purely geometric applications. In addition, the approach addresses certain requirements and limitations inherent in problems related to trajectory design for robot manipulators and not normally considered in problems of geometric design.

The effectiveness of the method in the examples discussed in Section 3 is an indication of the potential for improvement by making a careful choice of parametrization. Moreover, the importance of these results is not diminished by the absence of a uniqueness theorem for the higher dimensional case. The locally optimal solutions that may result from the application of the gradient projection method still provide improved parametrizations compared to the initial choice, excluding, of course, the exceptional case when the initial parametrization coincides with a relative minimum.

Acknowledgments

The author wishes to thank Drs. David Field and James Cavendish for their valuable comments and suggestions.

Note added in proof. The author has since learned that the problem considered in this paper was previously posed by Topfer in [10]. Also, subsequent work by Smith and Scherer [11] has resulted in a different uniqueness proof for the one-dimensional case.

References

1. T. N. E. Greville, Ed., "Theory and Application of Spline Functions," Academic Press, New York, 1969.
2. M. P. Epstein, On the influence of parametrization in parametric interpolation, *SIAM J. Numer. Anal.* **13** (2) (1976), 261.
3. C. deBoor, "A Practical Guide to Splines," Springer-Verlag, New York, 1978.
4. G. Mullineux, Approximating shapes using parameterized curves, *IMA J. Appl. Math.* **29** (2) (1982).
5. C.-S. Lin, P.-R. Chang, and J. Y. S. Luh, Formulation and optimization of cubic polynomial joint trajectories for mechanical manipulators, *in* "Proceedings of 21st IEEE Conference on Decision and Control, Orlando, Florida," December 8–10, 1982.

6. J. BOLLENGER AND N. DUFFIE, Computer algorithms for high speed continuous-path robot manipulation, *in* "Proceedings of the 29th General Assembly of the International Institute for Production Engineering Research, Davos, Switzerland," Aug. 26–Sept. 1, 1979, Hallwag, Berne, 1979.
7. C. W. EDWALL, H. J. POTTINGER, AND C. Y. HO, Trajectory generation and control of a robot arm using spline functions, *in* "Conference Proceedings, ROBOTS VI, Detroit, Michigan," March 2–4, 1982.
8. C. DEBOOR AND R. E. LYNCH, On splines and their minimum properties, *J. Math. Mech.* **15** (6) (1966).
9. DAVID G. LUENBERGER, "Introduction to Linear and Nonlinear Programming," Addison–Wesley, Reading, Mass., 1973.
10. H.-J. TOPFER, Models for smooth curve fitting, *in* "Conference Proceedings, Numerical Methods of Approximation Theory," Oberwolfach, FRG, January 19–23, 1981.
11. P. W. SMITH AND K. SCHERER, "Parametric Curve Fitting via Splines with Free Knots," unpublished manuscript.